Hartree-Fock-Bogoliubov mass models and the description of the neutron-star crust

Nicolas Chamel
in collaboration with S. Goriely and J. M. Pearson

Research Associate FNRS
Institute of Astronomy and Astrophysics
Université Libre de Bruxelles
Belgium

XXVIII International Workshop on Nuclear Theory, 22-27 June 2009, Rila Mountains, Bulgaria

LATEX

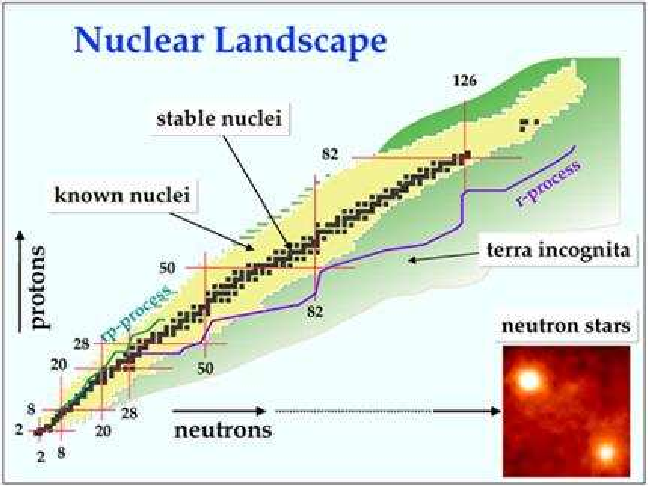

Punchline

The **self-consistent mean field theory** is a method of choice for the **global description** of various nuclear systems from finite nuclei to supernova core and neutron star crust

Outline

1. Mean field theory with effective interactions
   - HFB mass models
   - new effective interactions with improved pairing channel

2. Applications to the description of the neutron star crust
   - composition
   - neutron superfluidity

LaTeX

HFB mass models using effective interactions

The energy of a nucleus is expressed as ($q = n, p$ for neutrons,protons)

$$E = \int \mathcal{E}_{\rm HFB}\Big[\rho_q(\boldsymbol{r}), \boldsymbol{\nabla}\rho_q(\boldsymbol{r}), \tau_q(\boldsymbol{r}), \boldsymbol{J}_q(\boldsymbol{r}), \tilde{\rho}_q(\boldsymbol{r})\Big]\, {\rm d}^3\boldsymbol{r} + E_{\rm corr}$$

The various densities are calculated from $\varphi_{1k}^{(q)}(r)$ and $\varphi_{2k}^{(q)}(r)$

$$\begin{pmatrix} h_q(r) - \lambda_q & \Delta_q(r) \\ \Delta_q(r) & -h_q(r) + \lambda_q \end{pmatrix} \begin{pmatrix} \varphi_{1k}^{(q)}(r) \\ \varphi_{2k}^{(q)}(r) \end{pmatrix} = E_k^{(q)} \begin{pmatrix} \varphi_{1k}^{(q)}(r) \\ \varphi_{2k}^{(q)}(r) \end{pmatrix}$$

$$h_q \equiv -\boldsymbol{\nabla} \cdot \frac{\delta E_{\rm HFB}}{\delta \tau_q} \boldsymbol{\nabla} + \frac{\delta E_{\rm HFB}}{\delta \rho_q} - {\rm i} \frac{\delta E_{\rm HFB}}{\delta \boldsymbol{J}_q} \cdot \boldsymbol{\nabla} \times \boldsymbol{\sigma}$$

$$\Delta_q \equiv \frac{\delta E_{\rm HFB}}{\delta \tilde{\rho}_q}$$

Phenomenological corrections

$$E_{\mathrm{corr}} = E_W + E_{\mathrm{coll}}$$

- Wigner energy

$$E_W = V_W \exp\left\{-\lambda\left(\frac{N-Z}{A}\right)^2\right\} + V_W'|N-Z|\exp\left\{-\left(\frac{A}{A_0}\right)^2\right\}$$

- rotational and vibrational spurious collective energy

$$E_{\mathrm{coll}} = E_{\mathrm{rot}}^{\mathrm{crank}}\left\{b\ \tanh(c|\beta_2|) + d|\beta_2|\ \exp\{-l(|\beta_2| - \beta_2^0)^2\}\right\}$$

LaTeX

Determination of the model parameters

General fitting procedure

The parameters are fitted to the 2149 measured atomic masses with $Z, N \geq 8$

Additional constraints :

- isoscalar effective mass $M_s^*/M = 0.8$
- compressibility $230 \leq K_v \leq 270$ MeV
- charge radius of ^{208}Pb, $R_c = 5.501 \pm 0.001$ fm
- symmetry energy $J = 30$ MeV $\Leftrightarrow$ neutron-matter equation of state
- **NEW : $^1S_0$ pairing gap in infinite neutron matter**

LaTeX

Density dependent contact pairing force

$$v_q^{\text{pair}}(\boldsymbol{r_i},\boldsymbol{r_j}) = v^{\pi\, q}[\rho_n(\boldsymbol{r}),\rho_p(\boldsymbol{r})]\ \delta(\boldsymbol{r_i}-\boldsymbol{r_j}), \qquad \boldsymbol{r} = (\boldsymbol{r}_i+\boldsymbol{r}_j)/2$$

standard ansatz

$$v^{\pi\, q}[\rho_n,\rho_p] = V_{\pi q}\left(1-\eta\left(\frac{\rho_n+\rho_p}{\rho_0}\right)^{\alpha}\right)$$

Density dependent contact pairing force

$$v_q^{\text{pair}}(\boldsymbol{r_i},\boldsymbol{r_j}) = v^{\pi\, q}[\rho_n(\boldsymbol{r}),\rho_p(\boldsymbol{r})]\;\delta(\boldsymbol{r_i}-\boldsymbol{r_j}), \qquad \boldsymbol{r} = (\boldsymbol{r}_i+\boldsymbol{r}_j)/2$$

standard ansatz

$$v^{\pi\, q}[\rho_n,\rho_p] = V_{\pi q}\left(1-\eta\left(\frac{\rho_n+\rho_p}{\rho_0}\right)^{\alpha}\right)$$

Drawbacks

- not enough flexibility to fit realistic pairing gaps in infinite nuclear matter and in finite nuclei ($\Rightarrow$ isospin dependence)
- the fit is computationally expensive

LaTeX

Microscopically deduced pairing force

Assumptions :

- $v^{\pi\,q}[\rho_n, \rho_p] = v^{\pi\,q}[\rho_q]$ depends *only* on ρ_q
  Duguet, Phys. Rev. C 69 (2004) 054317.
- $v^{\pi\,q}[\rho_q]$ is the *locally* the same as in infinite nuclear matter with density ρ_q
- isospin charge symmetry $v^{\pi\,n} = v^{\pi\,p} = v^{\pi}$

Microscopically deduced pairing force

Assumptions :

- $v^{\pi\,q}[\rho_n, \rho_p] = v^{\pi\,q}[\rho_q]$ depends *only* on ρ_q
  Duguet, Phys. Rev. C 69 (2004) 054317.
- $v^{\pi\,q}[\rho_q]$ is the *locally* the same as in infinite nuclear matter with density ρ_q
- isospin charge symmetry $v^{\pi\,n} = v^{\pi\,p} = v^{\pi}$

New procedure

$v^{\pi}[\rho_q] = v^{\pi}[\Delta_n(\rho_q)]$ constructed so as to reproduce *exactly* a given pairing gap $\Delta_n(\rho_n)$ in neutron matter by solving *directly* the HFB equations in uniform neutron matter for each density ρ_n

Chamel, Goriely, Pearson, Nucl. Phys.A812,72 (2008).

LaTeX

Expression of the pairing force

Cutoff prescription : s.p. cutoff above the Fermi level

$$v^{\pi}[\rho_n] = -8\pi^2 \left(\frac{\hbar^2}{2M_n^*}\right)^{3/2} \left(\int_0^{\mu_n+\varepsilon_\Lambda} \mathrm{d}\varepsilon \frac{\sqrt{\varepsilon}}{\sqrt{(\varepsilon-\mu_n)^2+\Delta_n(\rho_n)^2}}\right)^{-1}$$

$$\mu_n = \frac{\hbar^2}{2M_n^*}(3\pi^2\rho_n)^{2/3}$$

Expression of the pairing force

Cutoff prescription : s.p. cutoff above the Fermi level

$$v^\pi[\rho_n] = -8\pi^2 \left(\frac{\hbar^2}{2M_n^*}\right)^{3/2} \left(\int_0^{\mu_n+\varepsilon_\Lambda} \mathrm{d}\varepsilon \frac{\sqrt{\varepsilon}}{\sqrt{(\varepsilon-\mu_n)^2+\Delta_n(\rho_n)^2}}\right)^{-1}$$

$$\mu_n = \frac{\hbar^2}{2M_n^*}(3\pi^2\rho_n)^{2/3}$$

- **exact** fit of the given gap $\Delta_n(\rho_n)$

Expression of the pairing force

Cutoff prescription : s.p. cutoff above the Fermi level

$$v^\pi[\rho_n] = -8\pi^2 \left(\frac{\hbar^2}{2M_n^*}\right)^{3/2} \left(\int_0^{\mu_n+\varepsilon_\Lambda} \mathrm{d}\varepsilon \frac{\sqrt{\varepsilon}}{\sqrt{(\varepsilon-\mu_n)^2+\Delta_n(\rho_n)^2}}\right)^{-1}$$

$$\mu_n = \frac{\hbar^2}{2M_n^*}(3\pi^2\rho_n)^{2/3}$$

- **exact** fit of the given gap $\Delta_n(\rho_n)$
- analytic expression **without any free parameters** !
- **automatic renormalization** of the pairing strength with any readjustments of the cutoff ε_Λ

Choice of the pairing gap

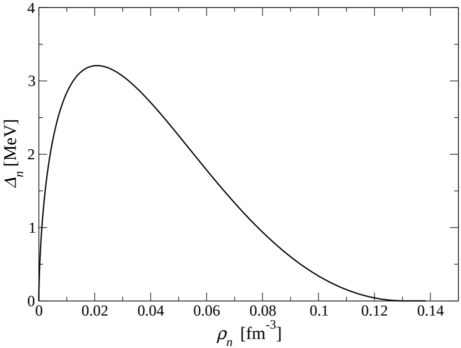

BCS pairing gap obtained with realistic nucleon-nucleon potentials

- $\Delta_n(\rho_n)$ essentially independent of the NN potential
- $\Delta_n(\rho_n)$ completely determined by experimental $^1S_0$ nn phase shifts

Dean&Hjorth-Jensen,Rev.Mod.Phys.75(2003)607.

Choice of the pairing cutoff

A priori the choice of ε_Λ is more or less arbitrary. But...

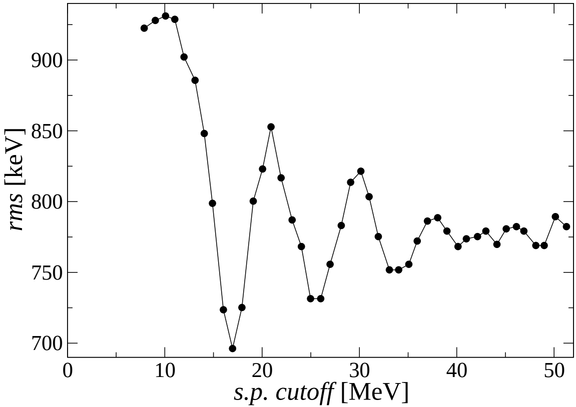

Goriely et al., Nucl.Phys.A773(2006),279

$\Rightarrow$ Best mass fits for $\varepsilon_\Lambda \simeq 16 - 17$ MeV

Neutron vs proton pairing

- Because of possible charge symmetry breaking effects, proton and neutron pairing strengths are not equal
- Neglect of polarization effects in odd nuclei (equal filling approximation) are corrected by “staggered” pairing

$\Rightarrow$ we introduce renormalization factors $f_q^{\pm}$ ($f_n^{+} \equiv 1$ by definition)

$$v^{\pi\, n}[\rho_n] = f_n^{\pm} v^{\pi}[\rho_n]$$

$$v^{\pi\, p}[\rho_p] = f_p^{\pm} v^{\pi}[\rho_p]$$

LaTeX

Neutron vs proton pairing

f_n^+	1.00
f_n^-	1.06
f_p^+	0.99
f_p^-	1.05

Note that $f_n^-/f_n^+ \simeq f_p^-/f_p^+$
$\Rightarrow$ neutron and proton pairing strengths are effectively equal

$\Rightarrow$ the pairing strength is larger for odd nuclei in agreement with a recent analysis by Bertsch et al. *Phys.Rev.C79(2009),034306*

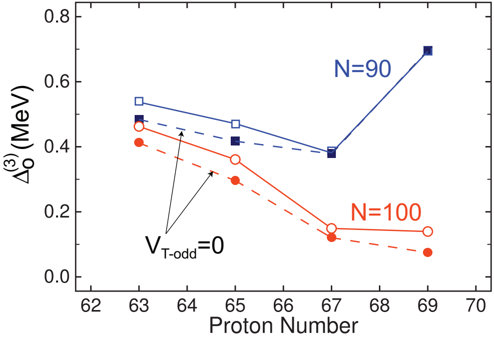

LaTeX

Nuclear matter properties predicted by the new Skyrme force BSk16

	BSk16	BSk15	BSk14
a_v [MeV]	-16.053	-16.037	-15.853
ρ_0 [fm^{-3}]	0.1586	0.1589	0.1586
J [MeV]	30.0	30.0	30.0
M_s^*/M	0.80	0.80	0.80
M_v^*/M	0.78	0.77	0.78
K_v [MeV]	241.6	241.5	239.3
L [MeV]	34.87	33.60	43.91
G_0	-0.65	-0.67	-0.63
$G_0^{'}$	0.51	0.54	0.51
G_1	1.52	1.47	1.49
$G_1^{'}$	0.44	0.41	0.44
ρ_{frmg}/ρ_0	1.24	1.24	1.24

Chamel, Goriely, Pearson, Nucl. Phys.A812,72 (2008).

LaTeX

Neutron-matter equation of state at subsaturation densities

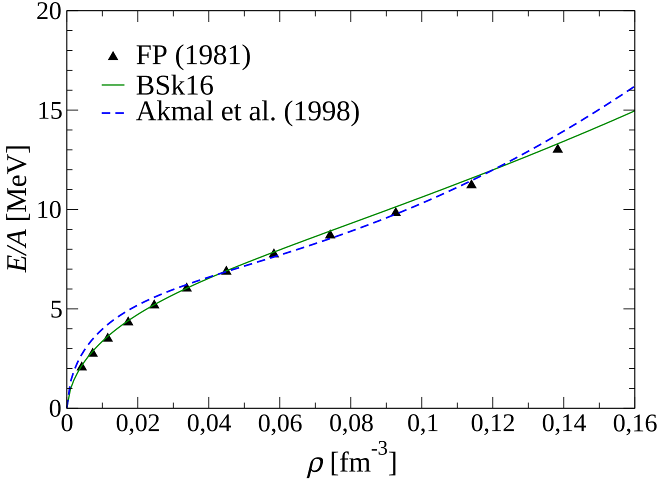

Chamel, Goriely, Pearson, Nucl. Phys.A812,72 (2008).

Neutron-matter equation of state at high densities

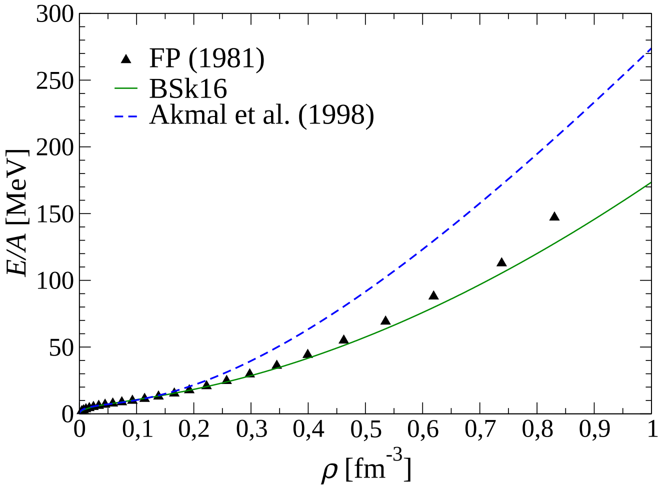

Chamel, Goriely, Pearson, Nucl. Phys.A812,72 (2008).

$^1S_0$ pairing gap in neutron matter

The new model yields a much more realistic gap than previous models !

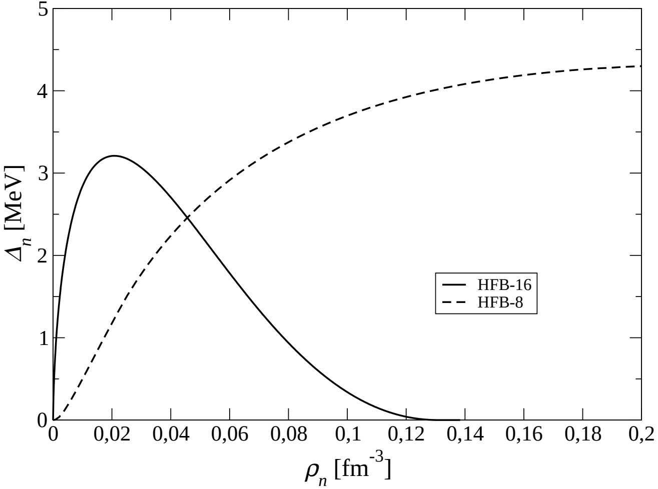

HFB-16 mass table

Results of the fit on the 2149 measured masses with $Z, N \geq 8$

	HFB-16	HFB-15	HFB-14	HFB-8
$\sigma(M)$ [MeV]	0.632	0.678	0.729	0.635
$\bar{\epsilon}(M)$ [MeV]	-0.001	0.026	-0.057	0.009
$\sigma(M_{nr})$ [MeV]	0.748	0.809	0.833	0.838
$\bar{\epsilon}(M_{nr})$ [MeV]	0.161	0.173	0.261	-0.025
$\sigma(S_n)$ [MeV]	0.500	0.588	0.640	0.564
$\bar{\epsilon}(S_n)$ [MeV]	-0.012	-0.004	-0.002	0.013
$\sigma(Q_\beta)$ [MeV]	0.559	0.693	0.754	0.704
$\bar{\epsilon}(Q_\beta)$ [MeV]	0.031	0.024	0.008	-0.027
$\sigma(R_c)$ [fm]	0.0313	0.0302	0.0309	0.0275
$\bar{\epsilon}(R_c)$ [fm]	-0.0149	-0.0108	-0.0117	0.0025
$\theta(^{208}\text{Pb})$ [fm]	0.15	0.15	0.16	0.12

Chamel, Goriely, Pearson, Nucl. Phys.A812,72 (2008).

LaTeX

BSk16 pairing predictions

Comparison of the experimental even-odd differences $\Delta^{(5)}$ with the HFB-16 theoretical neutron spectral pairing gaps $\langle uv\Delta\rangle$ for the Sn and Pb isotopic chains.

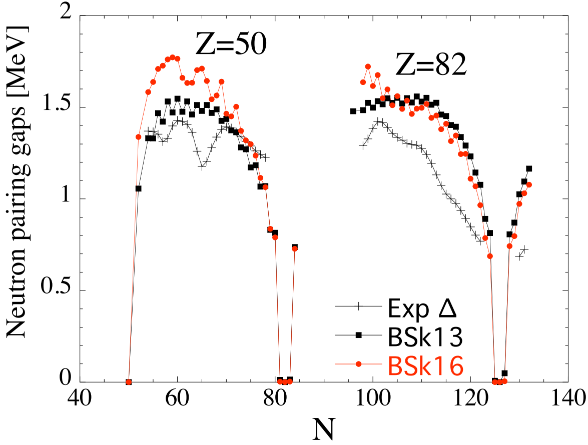

BSk16 pairing predictions

$N_0 = 50$ shell gap as function of Z for mass model HFB-16.

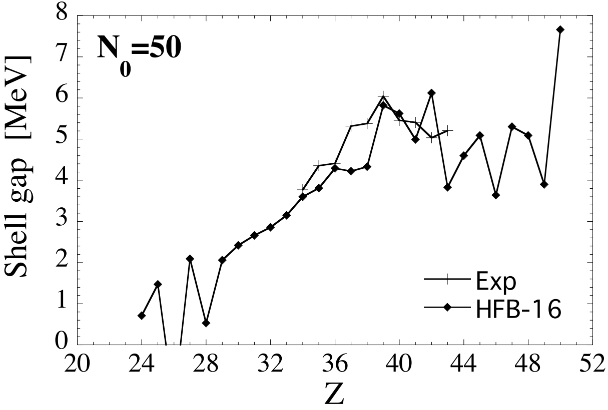

Chamel, Goriely, Pearson, Nucl. Phys.A812,72 (2008)

BSk16 pairing predictions

$N_0 = 82$ shell gap as function of Z for mass model HFB-16.

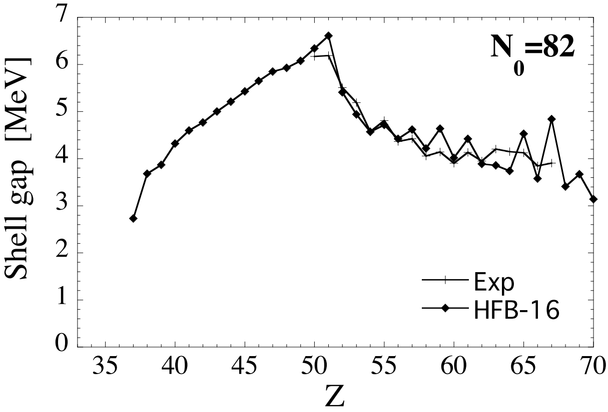

Chamel, Goriely, Pearson, Nucl. Phys.A812,72 (2008)

BSk16 pairing predictions

$N_0 = 126$ shell gap as function of Z for mass model HFB-16.

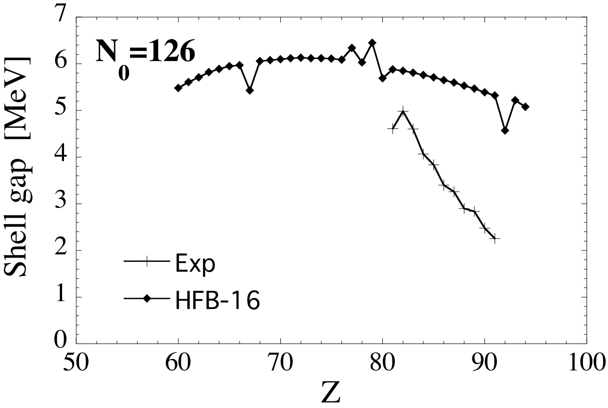

Chamel, Goriely, Pearson, Nucl. Phys.A812,72 (2008)

Latest mass model HFB-17

- Fit the $^1S_0$ pairing gaps of both neutron matter and symmetric nuclear matter
- include medium polarization effects on the gaps

Neutron matter

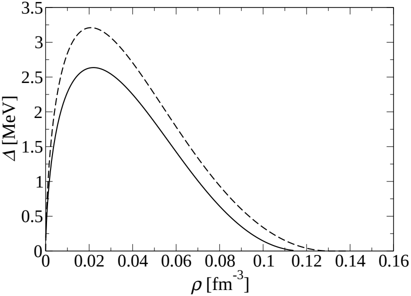

Symmetric nuclear matter

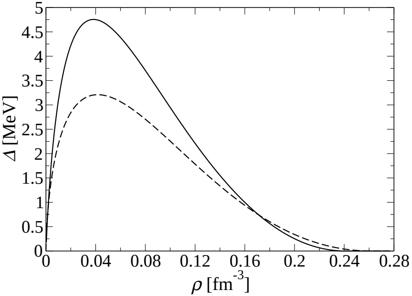

Pairing gaps from recent Brueckner calculations

Cao et al.,Phys.Rev.C74,064301(2006).

New expression of the pairing functional

- the pairing strength is allowed to depend on both ρ_n and ρ_p

$$v^{\pi\,q}[\rho_n, \rho_p] = v^{\pi\,q}[\Delta_q(\rho_n, \rho_p)]$$

- $\Delta_q(\rho_n, \rho_p)$ is interpolated between that of symmetric matter (SM) and pure neutron matter (NM)

$$\Delta_q(\rho_n, \rho_p) = \Delta_{SM}(\rho)(1 - |\eta|) \pm \Delta_{NM}(\rho_q)\,\eta\,\frac{\rho_q}{\rho}$$

- $M_q^* = M$ to be consistent with the neglect of self-energy effects on the gap

$$v^{\pi\,q}[\rho_n, \rho_p] = -8\pi^2 \left(\frac{\hbar^2}{2M}\right)^{3/2} \left(\int_0^{\mu_q+\varepsilon_\Lambda} \mathrm{d}\varepsilon \frac{\sqrt{\varepsilon}}{\sqrt{(\varepsilon-\mu_q)^2+\Delta_q^2}}\right)^{-1}$$

LaTeX

Density dependence of the pairing force

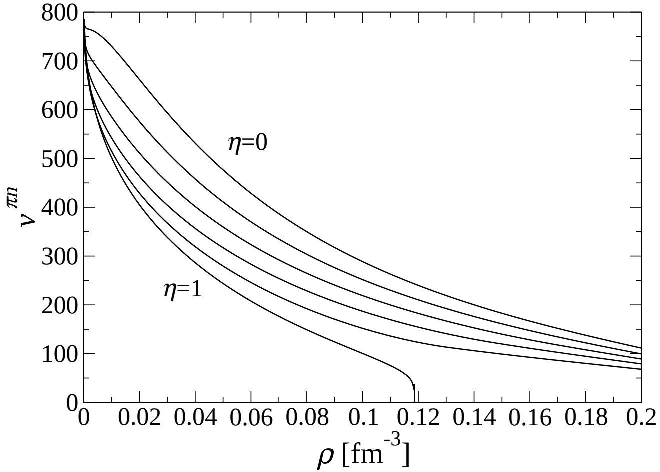

Goriely, Chamel, Pearson, EPJA (2009).

Isospin dependence of the pairing force

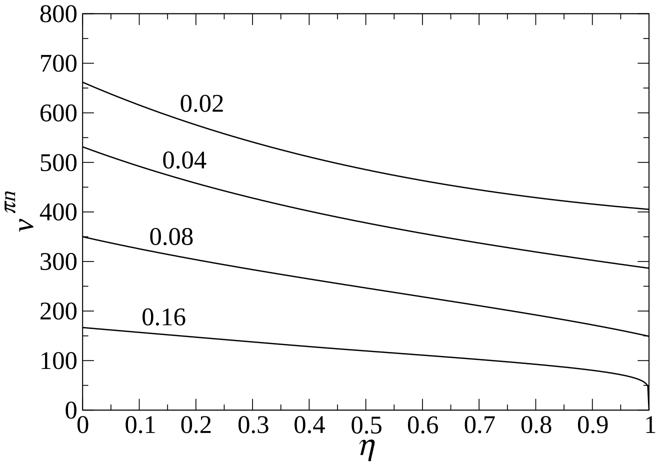

Goriely, Chamel, Pearson, EPJA (2009).

HFB-17 mass table

Results of the fit on the 2149 measured masses with $Z, N \geq 8$

	HFB-16	HFB-17
$\sigma(2149\ M)$	0.632	**0.581**
$\bar{\epsilon}(2149\ M)$	-0.001	-0.019
$\sigma(M_{nr})$	0.748	0.729
$\bar{\epsilon}(M_{nr})$	0.161	0.119
$\sigma(S_n)$	0.500	0.506
$\bar{\epsilon}(S_n)$	-0.012	-0.010
$\sigma(Q_\beta)$	0.559	0.583
$\bar{\epsilon}(Q_\beta)$	0.031	0.022
$\sigma(R_c)$	0.0313	0.0300
$\bar{\epsilon}(R_c)$	-0.0149	-0.0114
$\theta(^{208}\mathrm{Pb})$	0.15	0.15

Goriely, Chamel, Pearson, PRL102,152503 (2009).

HFB-17 mass predictions

Differences between experimental and calculated masses as a function of the neutron number N for the HFB-17 mass model.

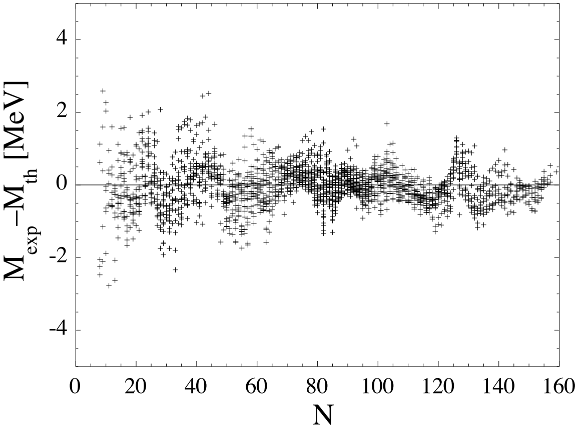

Goriely, Chamel, Pearson, PRL102,152503 (2009).

Predictions to newly measured atomic masses

HFB mass model fitted to the 2003 Atomic Mass Evaluation.
Compare its predictions to new measurements :

	HFB-16	HFB-17
$\sigma(434\ M)$	0.484	0.363
$\bar{\epsilon}(434\ M)$	-0.136	-0.092
$\sigma(142\ M)$	0.516	0.548
$\bar{\epsilon}(142\ M)$	-0.070	0.172

Litvinov et al., Nucl.Phys.A756, 3(2005)

http ://research.jyu.fi/igisol/JYFLTRAP_masses/ gs_masses.txt

LaTeX

Nuclear matter properties predicted by the new Skyrme force BSk17

	BSk16	BSk17
a_v	-16.053	-16.054
ρ_0	0.1586	0.1586
J	30.0	30.0
M_s^*/M	0.80	0.80
M_v^*/M	0.78	0.78
K_v	241.6	241.7
L	34.87	36.28
G_0	-0.65	-0.69
$G_0^{'}$	0.51	0.50
G_1	1.52	1.55
$G_1^{'}$	0.44	0.45
ρ_{frmg}/ρ_0	1.24	1.24

Goriely, Chamel, Pearson, PRL102,152503 (2009).

Comparison between HFB-16 and HFB-17

Differences between the HFB-16 and HFB-17 mass predictions as a function N for all $8 \leq Z \leq 110$ nuclei lying between the proton and neutron drip lines.

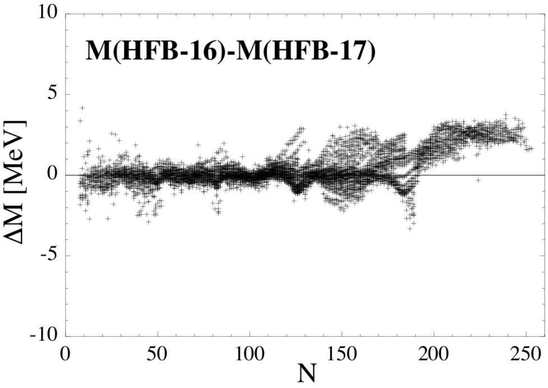

Goriely, Chamel, Pearson, EPJA (2009).

Neutron Stars

Neutron stars are the remnants of type II supernova explosions

Neutrons stars look like "very big" nuclei

For a ball of nuclear liquid

$$A \sim 10^{57} \qquad Z/A \sim 0.1$$

$$M \sim Am_p \sim 1 - 2M_\odot$$

$$R \sim r_0 A^{1/3} \sim 10 \text{ km}$$

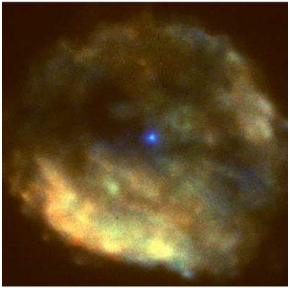

RCW 103 (from ESA)

Neutron star interiors

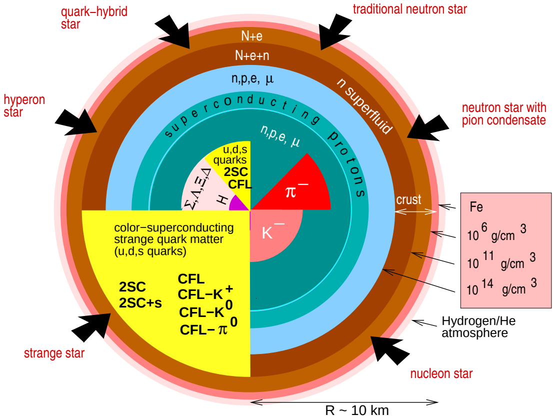

Picture from F. Weber

LaTeX

Neutron star crusts and observations

Many astrophysical phenomena are related to the physics of the neutron star crust

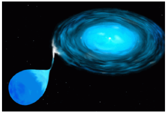

Thermonuclear burning in accreted crust
X-ray bursts and superbursts

EOS, neutrino transport
Supernova

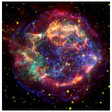

Magnetic crustquakes
Gamma ray bursts

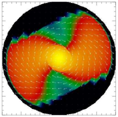

Non-axial deformations
(mountains, oscillations)
Gravitational waves

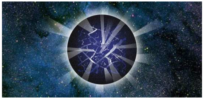

Neutron superfluid in the crust
Pulsar glitches

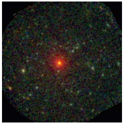

Neutron star cooling
Thermal X-ray emission

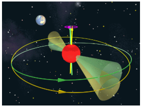

Crust elasticity, vortex pinning
Pulsar free precession

LATEX

Microscopic structure of neutron star crusts

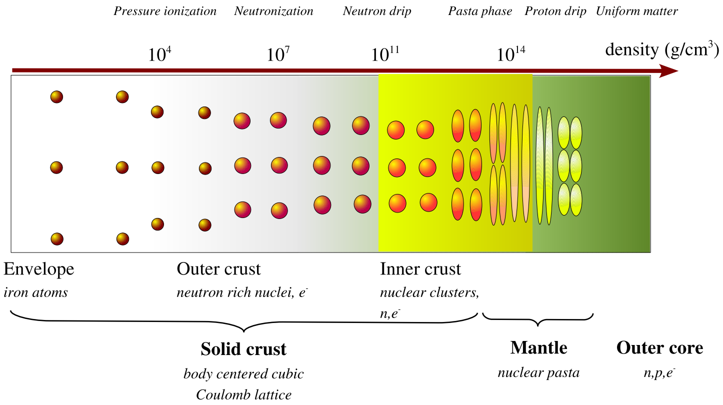

Chamel&Haensel, Living Reviews in Relativity 11 (2008), 10
http ://relativity.livingreviews.org/Articles/lrr-2008-10/

Various neutron star crusts

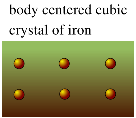

Low density cold catalyzed matter

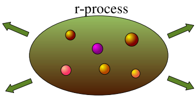

Ejected cold decompressed neutron star crust matter

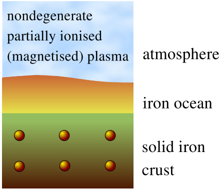

Weakly magnetised neutron star surface

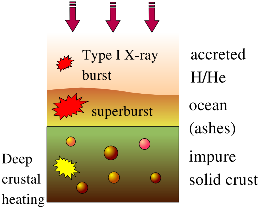

Accreting neutron star surface

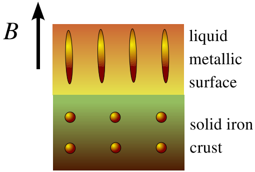

Strongly magnetised neutron star surface

Description of neutron star crust below neutron drip

Cold catalyzed matter

Harrison et al. (1965)

full thermodynamical equilibrium at $T = 0$

Description of neutron star crust below neutron drip

Cold catalyzed matter

Harrison et al. (1965)

full thermodynamical equilibrium at $T = 0$

Baym, Pethick, Sutherland (BPS), Astr. J.170(1971)299.

Perfect crystal with a single nuclear species (A,Z) at lattice sites

Description of neutron star crust below neutron drip

Cold catalyzed matter

Harrison et al. (1965)

full thermodynamical equilibrium at $T = 0$

Baym, Pethick, Sutherland (BPS), Astr. J.170(1971)299.

Perfect crystal with a single nuclear species (A,Z) at lattice sites

$\Rightarrow$ minimising the energy per nucleon ε/n_b

$$\varepsilon = n_N E\{A,Z\} + \varepsilon_e + \varepsilon_L$$

Description of neutron star crust below neutron drip

Cold catalyzed matter

Harrison et al. (1965)
full thermodynamical equilibrium at $T = 0$

Baym, Pethick, Sutherland (BPS), Astr. J.170(1971)299.
Perfect crystal with a single nuclear species (A,Z) at lattice sites
$\Rightarrow$ minimising the energy per nucleon ε/n_b

$$\varepsilon = n_N E\{A,Z\} + \varepsilon_e + \varepsilon_L$$

$E\{A,Z\}$ energy of a nucleus
ε_e energy density of the electron gas
ε_L lattice energy density

Description of neutron star crust below neutron drip

Cold catalyzed matter

Harrison et al. (1965)
full thermodynamical equilibrium at $T = 0$

Baym, Pethick, Sutherland (BPS), Astr. J.170(1971)299.
Perfect crystal with a single nuclear species (A,Z) at lattice sites
$\Rightarrow$ minimising the energy per nucleon ε / n_b

$$\varepsilon = n_N E\{A, Z\} + \varepsilon_e + \varepsilon_L$$

assuming a uniform relativistic electron gas
$\varepsilon_e = \frac{m_e^4 c^5}{8\pi^2 \hbar^3} \left(x(\sqrt{1+x^2}(1+2x^2) - \log\{x + \sqrt{1+x^2}\} \right)$
where $x = \hbar k_e / m_e c$ and $k_e = (3\pi^2 n_e)^{1/3}$

Description of neutron star crust below neutron drip

Cold catalyzed matter

Harrison et al. (1965)
full thermodynamical equilibrium at $T = 0$

Baym, Pethick, Sutherland (BPS), Astr. J.170(1971)299.
Perfect crystal with a single nuclear species (A,Z) at lattice sites
$\Rightarrow$ minimising the energy per nucleon ε/n_b

$$\varepsilon = n_N E\{A, Z\} + \varepsilon_e + \varepsilon_L$$

in a bcc lattice

$$\Rightarrow \varepsilon_L = -1.444 Z^{2/3} e^2 n_e^{4/3}$$

LaTeX

Composition of the neutron star outer crust

Using experimental masses when available

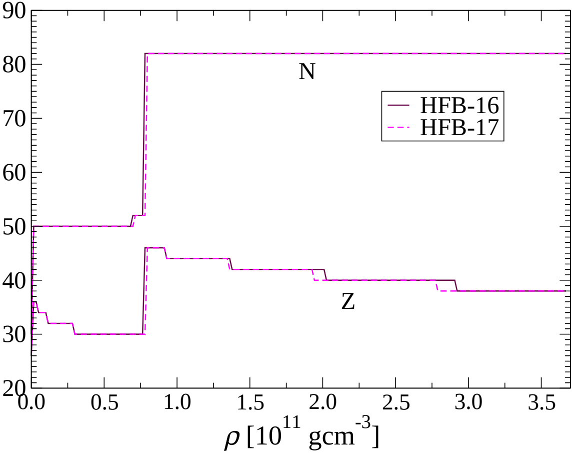

Goriely, Chamel, Pearson, EPJA (2009).

Description of the neutron star crust beyond neutron drip

Extended Thomas-Fermi+Strutinsky Integral (ETFSI) method

- Expand $\tau_q(\boldsymbol{r})$ and $\boldsymbol{J}_q(\boldsymbol{r})$ in terms of $\rho_q(\boldsymbol{r})$ and $\nabla\rho_q(\boldsymbol{r})$
- Minimize the energy per nucleon

$$\frac{E}{A} = \frac{\int \mathcal{E}_{\rm ETF}\Big[\rho_q(\boldsymbol{r}), \nabla\rho_q(\boldsymbol{r})\Big]\, {\rm d}^3\boldsymbol{r}}{\int \rho(\boldsymbol{r})\, {\rm d}^3\boldsymbol{r}}$$

- Include proton shell effects via the Strutinsky integral

$$E_p^{sc} = \sum_i n_i \widetilde{\epsilon_{i,p}} - \int d^3\mathbf{r}\left[\frac{\hbar^2}{\widetilde{2M_p^*}}\widetilde{\tau_p} + \widetilde{\rho_p}\widetilde{U_p} + \widetilde{\mathbf{J}_p}\cdot\widetilde{\mathbf{W}_p}\right]$$

Onsi et al., Phys.Rev.C77,065805 (2008).

Ground-state composition of the inner crust of neutron stars

Results of ETF+SI (and ETF) calculations with Skyrme BSk14

$\bar{\rho}$ (fm^{-3})	Z	A
0.0003	50 (38)	200 (146)
0.001	50 (39)	460 (385)
0.005	50 (39)	1140 (831)
0.01	40 (38)	1215 (1115)
0.02	40 (35)	1485 (1302)
0.03	40 (33)	1590 (1303)
0.04	40 (31)	1610 (1261)
0.05	20 (30)	800 (1171)
0.06	20 (29)	780(1105)

Onsi et al., Phys.Rev.C77,065805 (2008).

LaTeX

Equilibrium composition of the inner crust at finite temperature

Results of TETF+SI (and ETF) calculations with Skyrme BSk14
$T = 0.1$ MeV

$\bar{\rho}$ (fm^{-3})	Z	A
0.0003	50 (38)	200 (147)
0.001	50 (39)	460 (341)
0.005	50 (38)	1130 (842)
0.01	40 (38)	1210 (1107)
0.02	40 (35)	1480 (1294)
0.03	40 (33)	1595 (1303)
0.04	40 (31)	1610 (1242)
0.05	20 (30)	800 (1190)
0.06	20 (29)	765 (1116)

Onsi et al., Phys.Rev.C77,065805 (2008).

Equilibrium composition of the inner crust at finite temperature

Results of TETF+SI (and ETF) calculations with Skyrme BSk14

$T = 1$ MeV

$\bar{\rho}$ (fm^{-3})	Z	A
0.0003	46 (37)	310 (234)
0.001	46 (38)	520 (450)
0.005	44 (39)	1020 (858)
0.01	42 (37)	1280 (1120)
0.02	40 (36)	1480 (1307)
0.03	38 (33)	1505 (1301)
0.04	36 (31)	1450 (1232)
0.05	34 (30)	1340 (1165)
0.06	26 (29)	985 (1082)

$\Rightarrow$ disappearance of quantum shell effects

Onsi et al., Phys.Rev.C77,065805 (2008).

Sensitivity of the composition to the effective interaction

The composition of the inner crust depends strongly on the properties of the neutron ocean.

Example : Extended Thomas-Fermi calculations

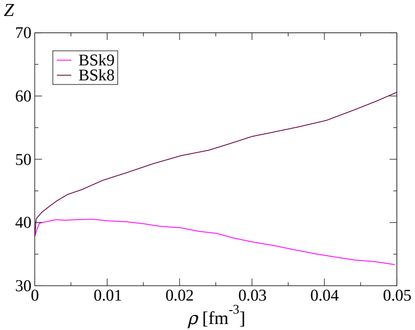

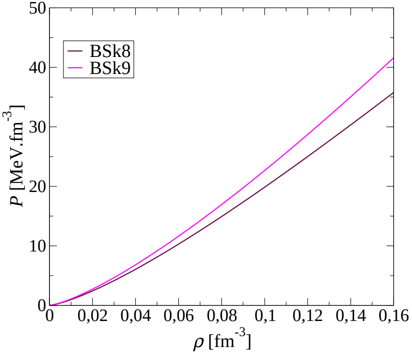

LATEX

HFB-14 vs HFB-17

Results of TETF+SI calculations with Skyrme BSk14

$\bar{\rho}$ (fm^{-3})	Z	A
0.0003	50	200
0.001	50	460
0.005	50	1140
0.01	40	1215
0.02	40	1485
0.03	40	1590
0.04	40	1610
0.05	20	800
0.06	20	780

HFB-14 vs HFB-17

Results of TETF+SI calculations with Skyrme BSk17

$\bar{\rho}$ (fm^{-3})	Z	A
0.0003	50	190
0.001	50	432
0.005	50	1022
0.01	50	1314
0.02	40	1258
0.03	40	1334
0.04	40	1354
0.05	40	1344
0.06	40	1308

LaTeX

Superfluidity in neutron star crust

Theoretically, neutron superfluidity in neutron star crust is well established.

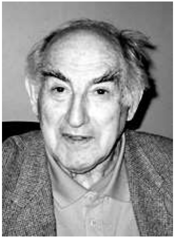

It was suggested long before the discovery of pulsars by Migdal (1959) only two years after BCS and studied by Ginzburg and Kirzhnits (1964), Wolff (1966) and many others

Superfluidity in neutron stars and observations

Observational evidence of superfluidity ?

- pulsar glitches (long relaxation times, glitch mechanism)
- neutron star thermal X-ray emission (cooling)

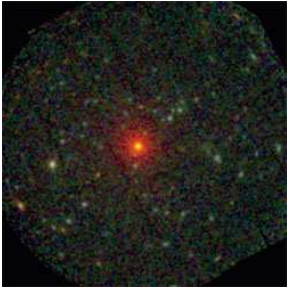

RXJ 0720.4-3125

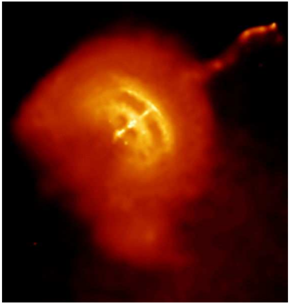

Vela pulsar

Effects of nuclear clusters on superfluidity ?

Most studies of superfluidity have been devoted to the case of pure neutron matter but...

Effects of nuclear clusters on superfluidity ?

Andersson's theorem

Effects of the clusters are negligible if the superfluid coherence length is much larger than the lattice spacing.

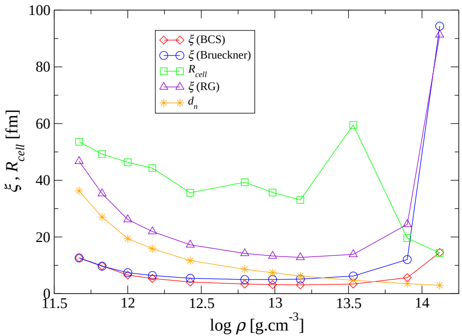

Pippard's definition

$$\xi = \frac{\hbar^2 k_{\rm F}}{\pi m_n \Delta}$$

based on the results of Negele&Vautherin

Superfluidity in the crust within the Wigner-Seitz approximation

The HFB equations have been already solved by several groups using the W-S approximation

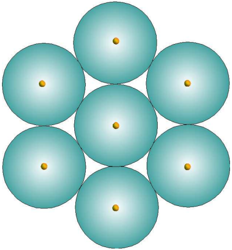

Superfluidity in the crust within the Wigner-Seitz approximation

The HFB equations have been already solved by several groups using the W-S approximation

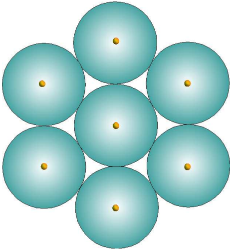

$\Rightarrow$ The effects of the clusters are found to be dramatic at high densities, in some cases the pairing gaps are almost completely suppressed!

Baldo et al., Eur.Phys.J. A 32, 97(2007).

Limitations of the W-S approximation

Problems

- the results depend on the boundary conditions which are not unique
- the nucleon densities and pairing fields exhibit spurious oscillations ($\Rightarrow$ shell effects) due to box-size effects

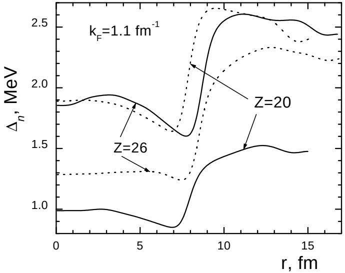

Baldo et al., Eur.Phys.J. A 32, 97(2007).

Limitations of the W-S approximation

Problems

- the results depend on the boundary conditions which are not unique
- the nucleon densities and pairing fields exhibit spurious oscillations ($\Rightarrow$ shell effects) due to box-size effects

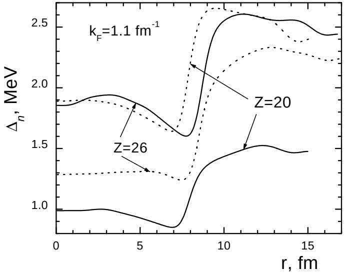

Baldo et al., Eur.Phys.J. A 32, 97(2007).

$\Rightarrow$ it is necessary to go beyond the W-S approach

Nuclear band theory

The inner crust of neutron stars is the nuclear analog of periodic systems in condensed matter : electrons in solids, photonic and phononic crystals, cold atomic Bose gases in optical lattice

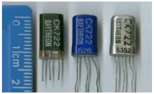

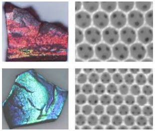

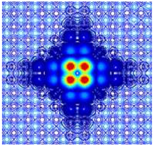

Nuclear band theory

The inner crust of neutron stars is the nuclear analog of periodic systems in condensed matter : electrons in solids, photonic and phononic crystals, cold atomic Bose gases in optical lattice

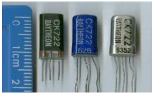

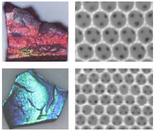

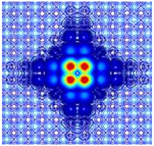

$\Rightarrow$ **nuclear band theory**

Chamel, Nucl.Phys.A747(2005)109.

Chamel, Nucl.Phys.A773(2006)263.

Chamel et al., Phys.Rev.C75(2007)055806.

Nuclear band theory

Floquet-Bloch theorem

> *« I found to my delight that the wave differed from the plane wave of free electrons only by a periodic modulation. »*

Bloch, Physics Today 29 (1976), 23-27.

$$\varphi_{\alpha\mathbf{k}}(\mathbf{r}) = e^{\mathrm{i}\mathbf{k}\cdot\mathbf{r}} u_{\alpha\mathbf{k}}(\mathbf{r})$$

$$u_{\alpha\mathbf{k}}(\mathbf{r}+\mathbf{T}) = u_{\alpha\mathbf{k}}(\mathbf{r})$$

- $\alpha \rightarrow$ rotational symmetry around the lattice sites
- $\mathbf{k} \rightarrow$ translational symmetry of the crystal

LaTeX

Symmetries

By symmetry, the crystal lattice can be partitionned into identical primitive cells.

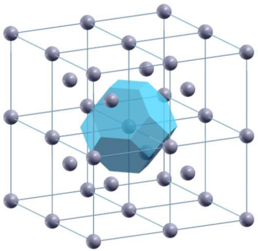

- The shape of the cell depends on the crystal symmetry
- The boundary conditions are fixed by the Floquet-Bloch theorem

$$\varphi_{\alpha\boldsymbol{k}}(\boldsymbol{r}+\boldsymbol{T}) = e^{i\boldsymbol{k}\cdot\boldsymbol{T}}\varphi_{\alpha\boldsymbol{k}}(\boldsymbol{r}) \Leftrightarrow u_{\alpha\boldsymbol{k}}(\boldsymbol{r}+\boldsymbol{T}) = u_{\alpha\boldsymbol{k}}(\boldsymbol{r})$$

Superfluidity in the inner crust beyond the W-S approximation

- Focus on bottom layers of the neutron star crust where the W-S approximation breaks down (also important for cooling and damping of inertial r-modes).
- Inhomogeneities near the crust-core transition are small $\Rightarrow$ "BCS approximation"

HFB equations in matrix representation

$$\begin{pmatrix} h-\lambda & \Delta \\ -\Delta^* & -h^*+\lambda \end{pmatrix} \begin{pmatrix} U \\ V \end{pmatrix} = E \begin{pmatrix} U \\ V \end{pmatrix}$$

$$h_{kl} = \int \mathrm{d}^3\boldsymbol{r}\, \phi_k^*(r) h_q(r)\, \phi_l(r)$$

$$\Delta_{kl} = \int \mathrm{d}^3\boldsymbol{r}\, \phi_k^*(r) \Delta_q(r) \phi_{\bar{l}}(r)$$

LaTeX

Superfluidity in the inner crust beyond the W-S approximation

- Focus on bottom layers of the neutron star crust where the W-S approximation breaks down (also important for cooling and damping of inertial r-modes).
- Inhomogeneities near the crust-core transition are small $\Rightarrow$ “BCS approximation”

If $\Delta(r)$ is slowly varying

$$\Delta_{kp} = \int \mathrm{d}^3\boldsymbol{r}\, \phi_k^*(r)\Delta(r)\phi_{\bar{p}}(r) \simeq \delta_{\bar{p}k}\Delta_k$$

Δ_k is the BCS pairing gap defined by

$$\Delta_k \equiv \int \mathrm{d}^3\boldsymbol{r}\, |\phi_k(r)|^2\Delta(r)$$

LaTeX

Validity of the BCS approximation

How good is the BCS approximation compared to HFB ?

valid whenever $\Delta(r)$ is slowly varying on the domain for which $\phi_k(r)$ around the Fermi level does not vanish (since only states around the Fermi level contribute to pairing).

- bad for weakly bound nuclei (delocalized continuum states involved while $\Delta_q(r)$ drop to zero outside nuclei)
- good for strongly bound nuclei
- exact for uniform matter

Validity of the BCS approximation

How good is the BCS approximation compared to HFB ?

valid whenever $\Delta(r)$ is slowly varying on the domain for which $\phi_k(r)$ around the Fermi level does not vanish (since only states around the Fermi level contribute to pairing).

- bad for weakly bound nuclei (delocalized continuum states involved while $\Delta_q(r)$ drop to zero outside nuclei)
- good for strongly bound nuclei
- exact for uniform matter

$\Rightarrow$ reasonable approx. for dense layers of neutron star crusts

Superfluidity in the inner crust beyond the W-S approximation

Generalized BCS equations to account for the periodic lattice

$$\Delta_{\alpha\boldsymbol{k}} = -\frac{1}{2}\sum_{\beta}\sum_{\boldsymbol{k'}} \bar{v}^{\rm pair}_{\alpha\boldsymbol{k}\alpha-\boldsymbol{k}\beta\boldsymbol{k'}\beta-\boldsymbol{k'}} \frac{\Delta_{\beta\boldsymbol{k'}}}{E_{\beta\boldsymbol{k'}}}\tanh\frac{E_{\beta\boldsymbol{k'}}}{2T}$$

$\Rightarrow$ analogy with terrestrial multi-band superconductors

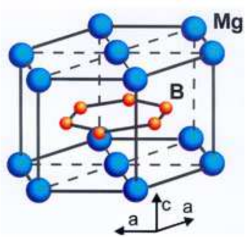

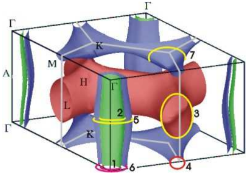

Multi-band superconductors were first studied by Suhl et al. in 1959 but clear evidence were found only in 2001 with the discovery of MgB_2

Composition of the neutron star crust

Nucleon density profiles from ETFSI calculations with BSk16 at $\rho = 10^{14}$ gcm^{-3}

Z=40, N=1220

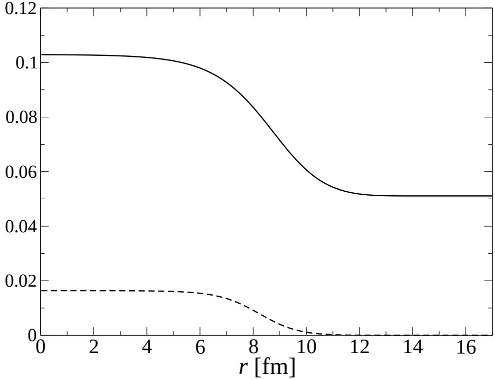

Neutron pairing gaps vs single-particle energies

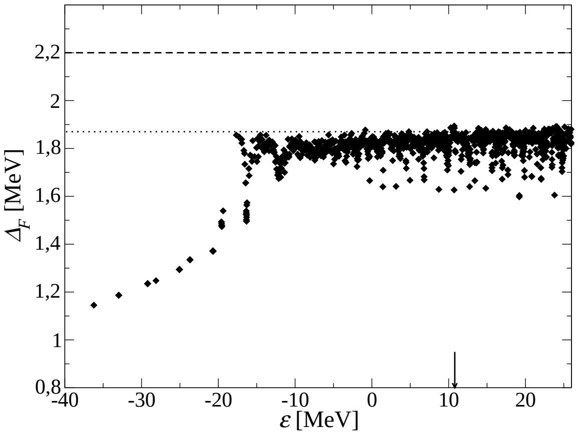

LATEX

Neutron pairing gaps vs single-particle energies

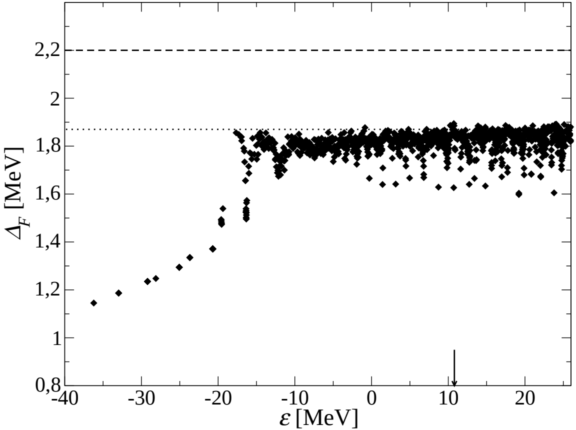

⇒ The presence of clusters reduces $\Delta_{\alpha\boldsymbol{k}}$ but much less than predicted by previous calculations

LaTeX

Average neutron pairing gap vs temperature

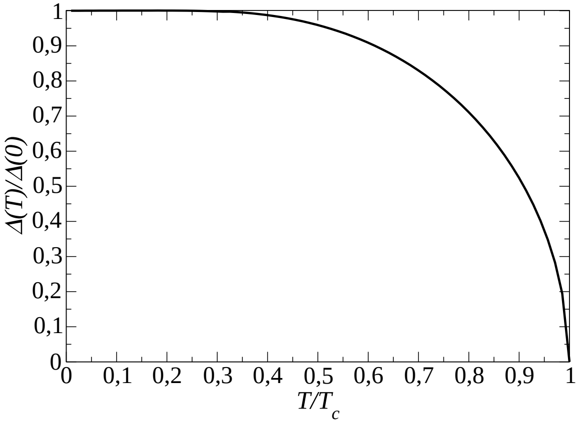

Average neutron pairing gap vs temperature

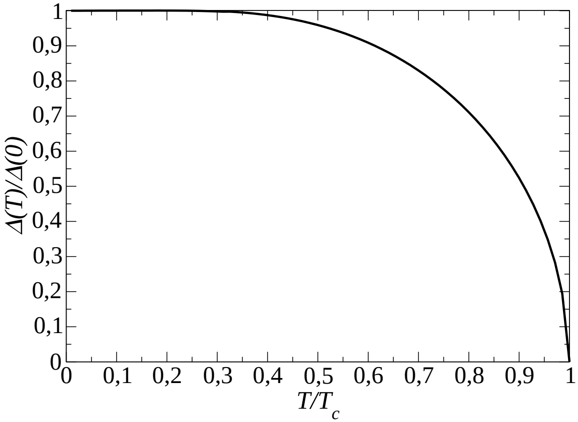

$\Rightarrow \Delta_{\alpha \boldsymbol{k}}(T)/\Delta_{\alpha \boldsymbol{k}}(0)$ is a universal function of T

Average neutron pairing gap vs temperature

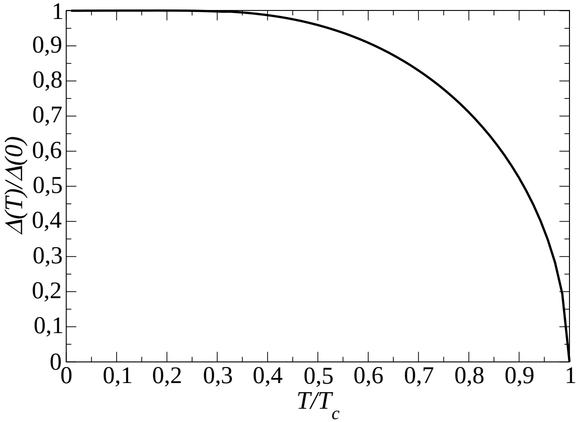

$\Rightarrow$ $\Delta_{\alpha\boldsymbol{k}}(T)/\Delta_{\alpha\boldsymbol{k}}(0)$ is a universal function of T

$\Rightarrow$ The critical temperature is approximately given by the BCS relation $T_{\rm c} \simeq \Delta_{\rm F}/1.76$

Specific heat of superfluid neutrons in neutron star crust

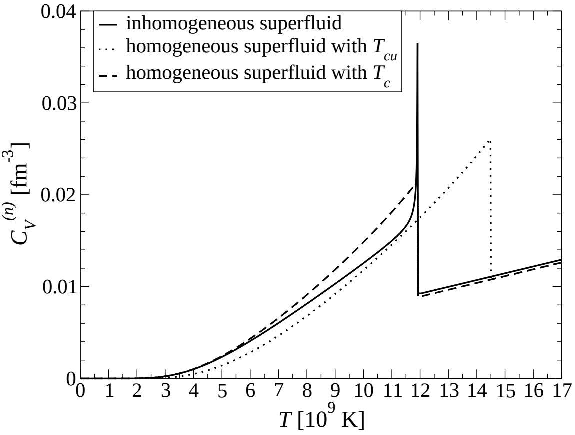

LATEX

Specific heat of superfluid neutrons in neutron star crust

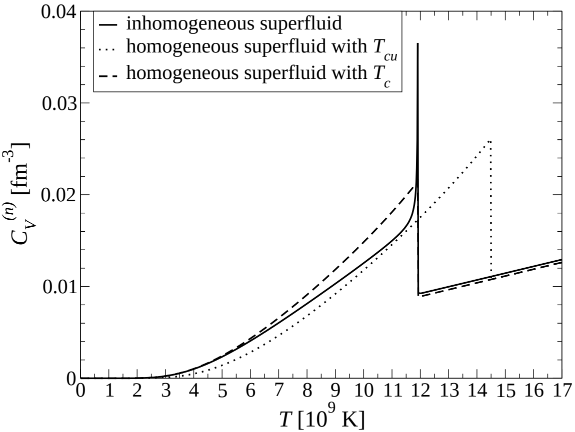

⇒ multi-band effects are small and $C_V^{(n)}$ is close to that of uniform neutron matter

Specific heat of superfluid neutrons in neutron star crust

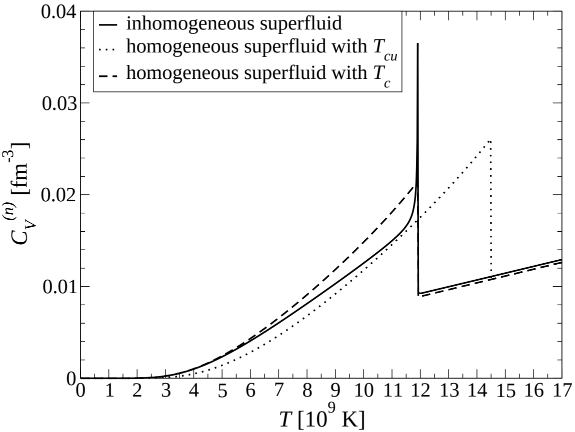

⇒ multi-band effects are small and $C_V^{(n)}$ is close to that of uniform neutron matter provided T_c is suitably renormalized

Dynamical effective mass and entrainment effects

Due to the interactions with the nuclear clusters, the neutrons move in the crust as if they had an effective mass $m_n^\star$.

For free electrons in solids

$$m_e^\star \sim 1 - 2m_e$$

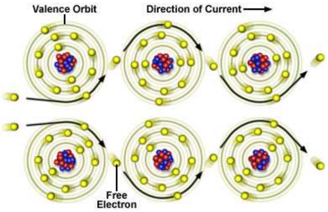

Dynamical effective mass and entrainment effects

Due to the interactions with the nuclear clusters, the neutrons move in the crust as if they had an effective mass $m_n^\star$.

For free electrons in solids

$$m_e^\star \sim 1 - 2m_e$$

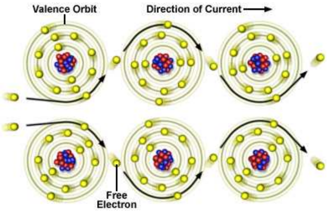

In the crust rest frame $\boldsymbol{p}_\mathbf{n} = m_n^\star \boldsymbol{v}_\mathbf{n}$ therefore in another frame

$$\boldsymbol{p}_\mathbf{n} = m_n^\star \boldsymbol{v}_\mathbf{n} + (m_n - m_n^\star)\boldsymbol{v}_\mathbf{c}$$

Dynamical effective mass and entrainment effects

Due to the interactions with the nuclear clusters, the neutrons move in the crust as if they had an effective mass $m_n^\star$.

For free electrons in solids

$$m_e^\star \sim 1 - 2m_e$$

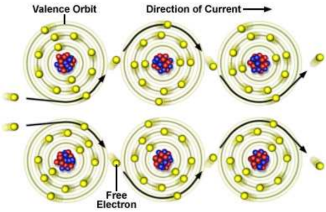

In the crust rest frame $\boldsymbol{p}_\mathbf{n} = m_n^\star \boldsymbol{v}_\mathbf{n}$ therefore in another frame

$$\boldsymbol{p}_\mathbf{n} = m_n^\star \boldsymbol{v}_\mathbf{n} + (m_n - m_n^\star)\boldsymbol{v}_\mathbf{c}$$

$\Rightarrow$ entrainment effects are important for neutron star dynamics (oscillations, precession, glitches)

Dynamical effective neutron mass in the crust

Using the band theory of solids, $m_\star^n$ is given by

$$m_\star^n = \frac{n_n}{\mathcal{K}} \qquad \mathcal{K} = \frac{1}{3}\int_F \frac{\mathrm{d}^3k}{(2\pi)^3}\,\mathrm{Tr}\frac{1}{m_\star^n(\boldsymbol{k})}$$

with the usual local effective mass tensor defined by

$$\left(\frac{1}{m_\star^n(\boldsymbol{k})}\right)^{ij} = \frac{1}{\hbar^2}\frac{\partial^2 \mathcal{E}_{\boldsymbol{k}}}{\partial k_i \partial k_j}\,.$$

Note that this has been also applied in neutron diffraction
Zeilinger et al., PRL57 (1986), 3089.

Neutron Fermi surface

The dynamical effective mass arises from distorsions of the Fermi surface

isolated ^{91}Zr (electron FS)

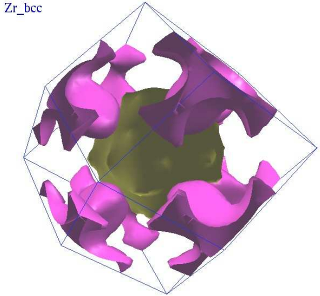

^{200}Zr in NS crust (neutron FS)

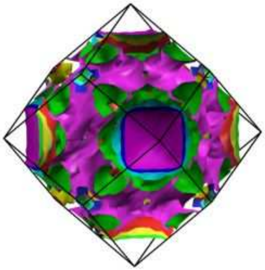

LaTeX

Dynamical effective neutron mass in the neutron star crust

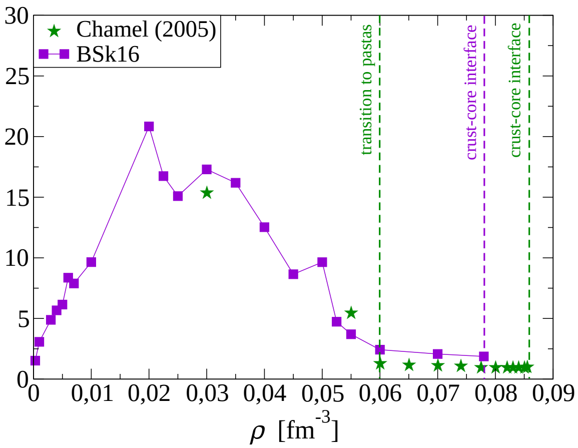

Chamel, Nucl.Phys.A749, 107 (2005)
Preliminary results for BSk16

LATEX

Quasi-periodic oscillations in Soft-Gamma Repeaters

Detection of QPOs in giant flares of several SGR

Example : SGR 1806−20

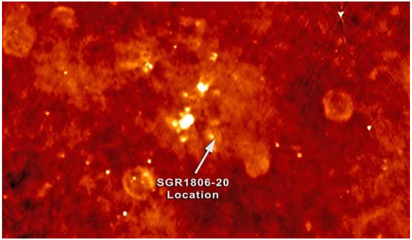

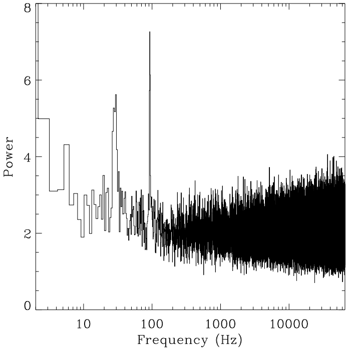

Quasi-periodic oscillations in Soft-Gamma Repeaters

Detection of QPOs in giant flares of several SGR

- SGR 1806$-$20 (27 December 2004)
  18, 26, 29, 92.5, 150, 626.5 and 1837 Hz
  Israel et al., ApJ 628 (2005),53
  Watts et al., ApJ 637 (2006),117
  Strohmayer et al., ApJ 653 (2006),593
- SGR 1900$+$14 (27 August 1998)
  28, 54, 84 and 155 Hz
  Strohmayer et al., ApJ 632 (2005),111
- SGR 0526$-$66 (5 March 1979)
  43.5 Hz
  Barat et al., A&A 126 (1983),400.

Magnetar model

SGR are believed to be strongly magnetized neutron stars

QPOs are interpreted as seismic vibrations following magnetic crustquakes

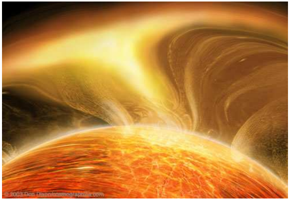

If confirmed, this would be the first direct observation of NS oscillations !

LaTeX

Magnetar seismology

The frequencies of the seismic modes depend on the internal structure of the neutron star. In particular the modes are affected by the neutron superfluid in the crust (effective mass)

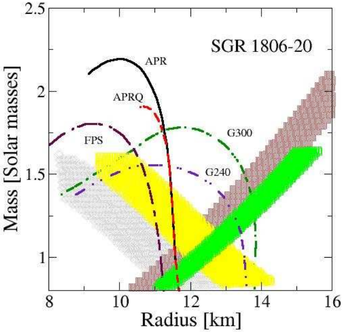

From Lars Samuelsson

Summary

- We have developed effective nucleon forces that are very well-suited for astrophysics applications :
  - they give an excellent fit to essentially all nuclear mass data ($\sigma = 581$ keV for HFB-17) *http ://www.astro.ulb.ac.be/Html/bruslib.html*
  - they reproduce the neutron matter eos and $^1S_0$ pairing gap obtained with realistic potentials (among other things).
- We have just started to apply them for calculating the properties of neutron star crust using new methods from solid state physics :
  - composition, equation of state
  - neutron pairing gaps, effective mass

LaTeX

Perspectives

- Improve the nuclear functional :
  - ▷ remove spurious instabilities (ex. ferromagnetic transition) at low densities
  - ▷ include in the mass fit additional microscopic constraints in the spin-isospin channel
- A few open issues in the neutron star crust physics :
  - ▷ Existence of nuclear pastas ?
  - ▷ Many-body effects on superfluidity ?
  - ▷ Impact of strong magnetic fields ?
  - ▷ Deviations from ground-state composition ?